Journal of Molecular Medicine
https://doi.org/10.1007/s00109-021-02176-x

ORIGINAL ARTICLE

Recapitulating lipid accumulation and related metabolic dysregulation in human liver-derived organoids

Ling Wang[1] · Meng Li[1,4] · Bingting Yu[1] · Shaojun Shi[2] · Jiaye Liu[1] · Ruyi Zhang[1] · Ibrahim Ayada[1] · Monique M. A. Verstegen[2] · Luc J. W. van der Laan[2] · Maikel P. Peppelenbosch[1] · Wanlu Cao[3] · Qiuwei Pan[1]

Received: 12 July 2021 / Revised: 17 December 2021 / Accepted: 20 December 2021

Abstract

Fatty liver disease has grown into a major global health burden, attributed to multi-factors including sedentary lifestyle, obesogenic diet and prevalence of metabolic disorders. The lack of robust experimental models is hampering the research and therapeutic development for fatty liver disease. This study aims to develop an organoid-based 3D culture model to recapitulate key features of fatty liver disease focusing on intracellular lipid accumulation and metabolic dysregulation. We used human liver-derived intrahepatic cholangiocyte organoids and hepatocyte differentiated organoids. These organoids were exposed to lactate, pyruvate, and octanoic acid (LPO) for inducing lipid accumulation and mitochondrial impairment. Lipid accumulation resulted in alternations of gene transcription with major effects on metabolic pathways, including triglyceride and glucose level increase, which is consistent with metabolic changes in fatty liver disease patients. Interestingly, lipid accumulation affected mitochondria as shown by morphological transitions, alternations in expression of mitochondrial encoded genes, and reduction of ATP production. Meanwhile, we found treatment with obeticholic acid and metformin can alleviate fat accumulation in organoids. This study demonstrated that LPO exposure can induce lipid accumulation and associated metabolic dysregulation in human liver-derived organoids. This provides an innovative model for studying fatty liver disease and testing potential therapeutics.

Key messages

- Lactate, pyruvate, and octanoic acid induce lipid accumulation in liver organoids.
- Organoids of human compared to mouse origin are more efficient in lipid accumulation.
- Lipid accumulation dysregulates metabolic pathway and impairs mitochondrial function.
- Demonstrating a proof-of-concept for testing medications in organoids.

Keywords Fatty liver disease · Liver organoids · Lipid accumulation · Metabolic dysregulation

Abbreviations

NAFLD	Non-alcoholic fatty liver disease
MAFLD	Metabolic dysfunction associated fatty liver disease
ICOs	Intrahepatic cholangiocyte organoids
LPO	Lactate, pyruvate, and octanoic acid
TMRM	Tetramethylrhodamine
PLIN 1	Perilipin 1
PLIN2	Perilipin 2
PPARα	Peroxisome proliferator-activated receptor alpha
CPT1A	Carnitine palmitoyltransferase 1A
PCK1	Phosphoenolpyruvate carboxykinase 1
G6PC	Glucose-6-phosphatase
HSD17B13	17β-Hydroxysteroid dehydrogenase type 13

✉ Wanlu Cao
wanlu724576084@hotmail.com

✉ Qiuwei Pan
q.pan@erasmusmc.nl

[1] Department of Gastroenterology and Hepatology, Erasmus MC-University Medical Center, Rotterdam, The Netherlands

[2] Department of Surgery, Erasmus MC-University Medical Center, Rotterdam, The Netherlands

[3] Department of Oncology, Shanghai East Hospital, Tongji University, Shanghai, China

[4] Guangzhou Institutes of Biomedicine and Health, Chinese Academy of Sciences, Guangzhou 510530, China

Published online: 20 January 2022

CHREBP	Carbohydrate-responsive element-binding protein
LXR α	Liver X receptor alpha
TGFB1	Transforming growth factor beta 1
SCL25A4	Solute carrier family 25, member 4
PGC1 α	Peroxisome proliferator-activated receptor-gamma coactivator 1 alpha
OXPHOS	Oxidative phosphorylation
ATP	Adenosine triphosphate
CK7	Cytokeratin 7
CK19	Cytokeratin 19
HNF4α	Hepatocyte nuclear factor 4 alpha
OCT4	Octamer-binding transcription factor 4
LGR5	Leucine-rich repeat containing G protein-coupled receptor 5
B2M	Beta2-microglobulin

Introduction

Non-alcoholic fatty liver disease (NAFLD) is one of the most common chronic liver diseases, affecting approximately one-third of the global population. Attributing to dietary and life style changes; the global incidence of NAFLD is continuously growing. It includes simple steatosis and nonalcoholic steatohepatitis, which accompanies with inflammation. Although the disease in majority of individuals is simple steatosis that can be improved by lifestyle modifications and physical activity increase, a subset of patients with inflammation can develop serious complications, including fibrosis, cirrhosis and liver cancer [1]. Recently, the nomenclature of NAFLD has been proposed to be updated as metabolic dysfunction associated fatty liver disease (MAFLD) [2]. In addition to hepatic steatosis, the MAFLD criteria also emphasize metabolic dysfunctions, including the presence of type II diabetes mellitus, overweight/obesity, or minimal two minor metabolic abnormalities. Currently, research on the etiology and pathogenesis of fatty liver disease remains at infancy, and there is no approved medication available.

Extra fat storage in the liver is a hallmark of fatty liver disease. It can present as lipid droplets primarily in hepatocytes [3]. Lipid accumulation may also occur in cholangiocytes under specific circumstances. For example, lipid droplets were observed in cholangiocytes in Comparative Gene Identification-58 (CGI-58), a lipid droplet-associated gene, knockout mice, fed a Western diet. Mutations in this gene are known to manifest fatty liver disease in humans and rodents [4]. To model the process of steatosis in vitro, several human liver cancer cell lines such as human hepatoblastoma-based cell lines have been used [5]. It has been demonstrated that combinatory supplementation of lactate, pyruvate, and octanoic acid (LPO) can stimulate lipid synthesis in cell culture, resembling a fatty liver disease phenotype [5]. However, these cancer cell lines have been passaged in cell culture for decades, and harbor various genetic, epigenetic, and functional alterations [6]. Therefore, they have fundamental limitations in modeling fatty liver disease. Thus, advancing mechanistic understanding of this disease and developing therapeutics require innovative and robust experimental models. The organoid technology has provided a unique tool to circumvent these limitations. Organoids generated from human induced pluripotent stem cells have been explored for modeling steatosis and other liver diseases [7, 8]. Importantly, primary organoids can be cultured from tissue stem cells in 3D structure, and they are much better in recapitulating the characteristics of the tissue of origin [9].

Human and mouse livers harbor residential bipotent progenitor cells located in the intrahepatic biliary compartment that can be cultured as organoids [10, 11]. These liver organoids are derived from intrahepatic bile ducts, thus also termed as intrahepatic cholangiocyte organoids (ICOs) [12], which have been well-characterized [13]. ICOs can be differentiated toward a hepatocyte-like phenotype by defined culture conditions [10] and can be maintained in culture for a period of time [14]. In this study, we aim to recapitulate lipid accumulation and associated metabolic dysregulation, and to test medications on lipid accumulation in liver organoids.

Materials and methods

Liver organoids culture

Human liver organoids (ICOs) were isolated and cultured as previously described [15]. Liver organoids were cultured with Advanced DMEM/F12 (Life Technologies, cat.no.12634–010), adding 1 M HEPEs (Lonza, cat. no. 17-737E) and ultraglutamine (Lonza, cat. no. BE17-605E/U1) as the basic culture medium, supplied with 1:50 B27 supplement (minus vitamin A), 1:100 N2 supplement, 1 mM N-acetylcysteine, 10 mM nicotinamide, 50 ng/ml EGF, 100 ng/ml FGF-10, 50 ng/ml HGF, 5 µM A83-01, 10 µM forskolin, 10 nM gastrin, and 10% R-spondin1 (produced by 293 T-H-RspoI-Fc cell line). The use of human liver tissues for research purposes was approved by the Medical Ethical Council of Erasmus MC and informed consent was given (MEC-2014–060).

Hepatocyte differentiation of human ICOs

Hepatocyte differentiation of human ICOs has been well-described previously [15]. Briefly, after culturing with human liver organoids expansion medium supplemented with BMP7 (25 ng/ml) for 5 days, the culture condition was changed to hepatocyte differentiation medium. The differentiation medium is the basic culture medium

supplemented with 1:50 B27 supplement, 1:100 N2 supplement, 1 mM N-acetylcysteine, 10 nM gastrin, 50 ng/ml EGF, 25 ng/ml HGF, 0.5 μM A83-01, 10 μM DAPT, 3 μM dexamethasone, 25 ng/ml BMP7, and 100 ng/ml FGF19.

Induction of lipid accumulation

According to the previously described protocol [16], lactate (L), pyruvate (P), and octanoic acid (O) (all from Sigma-Aldrich, UK) were added in organoid culture medium. Low (L:P:O: 10 mM: 1 mM: 2 mM) and high (L:P:O: 15 mM: 1.5 mM: 3 mM) concentrations were used. Culture medium was refreshed every 2 days.

Alamar Blue assay

Culture supernatant of organoids was first discarded. Organoids were then incubated with Alamar Blue (Invitrogen, DAL1100, 1:20 dilution in OEM) for two hours at 37 °C. The medium was collected for analyzing cell viability. Absorbance was measured by fluorescence plate reader at the excitation of 530/25 nm and emission of 590/35 nm.

Cell cycle analysis

Organoids were collected and dissociated into single cells by using 0.05% Trypsin–EDTA, followed by washing twice with 1X PBS and fixing in cold 70% ethanol overnight at –20 °C. The cells were washed twice with PBS and incubated with 100 μg/ml RNase A at 37 °C for 30 min, and then 50 μg/ml propidium iodide (PI) was added and incubated at 4 °C for 30 min. The samples were analyzed by FACS Calibur. Cell cycle was analyzed by FlowJo_V10 software.

Apoptosis analysis

Apoptosis was measured by Annexin V-FITC/PI apoptosis detection kit (Becton Dickinson). Experiments were performed according to the manufacturer's instruction. Briefly, organoids were treated by TrypLE express for dissociation into single cells and washed with cold PBS. Samples were incubated with mixture of 1X Binding buffer, FITC Annexin V, and PI for 15 min at room temperature in the dark. The samples were then measured by FACS. Cell apoptosis rate was analyzed by FlowJo_V10 software.

Staining of lipids

Lipids were stained with AdipoRed (Lonza, cat.no.PT-7009) and Hoechst 33342 (Life Technologies, cat.no.H3570) for 30 min, followed by washing with 1X PBS 3 times. Images were captured by confocal microscope Zeiss LSM510meta and Leica SP5, and quantified with ImageJ software. Analysis was performed by splitting the individual color channel for lipids and threshold converting the 8-bit. The acquired images were measured with particles and their surface areas in pixels, then converted to square micrometers for areas of lipid droplets.

Co-staining of lipid and mitochondria

Mitochondria were stained with tetramethylrhodamine (TMRM) (Life Technologies, cat. no. T668), lipids were stained with monodansylpentane (MDH) (Abgent, cat. no. SM1000b), and nucleus were stained with DRAQ5 (Fisher Scientific, cat. no. 62251) for 30 min. The images were captured by confocal microscope Zeiss LSM510meta and Leica SP5, and quantified with ImageJ software.

Immunofluorescence staining of organoids

Organoids were collected and fixed by formalin (4%) for 10 min. The samples were washed and blocked for 1 h. Subsequently, samples were incubated with primary antibodies against Albumin (Sigma-Aldrich, cat. no. A6684) and CK7 (Invitrogen, cat. no. MA1-06,316) overnight at 4°C. After washing, samples were incubated with secondary antibody (Invitrogen, cat. no. A32742) for 1 h at room temperature. Then DAPI (Fisher Scientific, cat. no. 13285184) was added to stain nucleus. Images were captured by confocal microscope Leica SP5.

Triglyceride assay

EnzyChrom™ Triglyceride Assay Kit (BioAssay Systems, cat. no. ETGA-200) was used to measure triglyceride content according to previously described protocol [7]. Organoids were collected and seeded in 96-well plate for 3 days treated or untreated with LPO, and then working reagent was added for each well incubated for 30 min at room temperature. Absorbance was measured by absorbance microplate reader Infinite® M Nano at 570 nm. The final results were normalized to total protein concentration of the organoids.

Diacyglycerol assay

Diacylglycerol assay kit (Cell Biolabs, cat. no. MET-5028) was used to measure diacylglycerol content according to manufacturer's introduction. Organoids were harvested and sonicated on ice to extract diacylglycerol. Then samples were transferred to a 96-well microtiter plate. Reagents were added and incubated at room temperature for 10 min. Absorbance was measured by fluorescence plate reader at the excitation of 530/25 nm and emission of 590/35 nm. The final results were normalized to total protein concentration of the organoids.

Glucose assay

Glucose Assay Kit (Abcam, cat.no.ab65333) was used to measure glucose content. Organoids were collected after 96 h treated or untreated with LPO, and then working reagent was added according to the instruction. Absorbance was measured by absorbance microplate reader Infinite® M Nano at 570 nm. The final results were normalized to total protein concentration of the organoids.

Measurement of ATP content

Organoids were collected after LPO exposure. Organoids were divided equally into two tubes for ATP test and total protein concentration measurement. ATP Bioluminescence Assay Kit CLS II (Sigma-Aldrich, cat. no. 11699695001) was used for ATP content measurement. The final results were normalized by total protein concentration of the organoids.

RNA isolation and sequencing

Total RNA of cultured organoids was isolated using Machery-NucleoSpin RNA Kit (Bioke, cat. no. MN 740955.250) and quantified by Nanodrop 2000. The quality of RNA was measured by Bioanalyzer RNA 6000 Picochip as quality-control step, followed by RNA sequencing performed by Novogene with paired-end 150 bp (PE 150) sequencing strategy. The identification of differentially expressed genes was based on $P < 0.05$ and absolute values of $\log_2 Fc > 1$.

qRT-PCR

Total RNA of cultured organoids was isolated using Machery-NucleoSpin RNA Kit (Bioke, cat. no. MN 740955.250) and quantified by Nanodrop 2000. Reverse transcription was produced by PrimeScript RT Master Mix (Takara Bio Inc., cat. no. RR036B). qRT-PCR was performed with SYBR Select Master Mix (Life Technologies, cat. no. 4472954) with the StepOnePlus System (Thermo Fisher Scientific Life Sciences). Beta2-microglobulin (B2M) gene served as a reference. Relative gene expression of the target gene was normalized to the reference using the formula $2^{-\Delta\Delta CT}$ ($\Delta\Delta CT = \Delta CT$sample—$\Delta CT$control). These genes include perilipin 1 (PLIN1), perilipin 2 (PLIN2), glucose-6-phosphatase (G6PC), peroxisome proliferator-activated receptor alpha (PPARα), carnitine palmitoyltransferase 1A (CPT1A), phosphoenolpyruvate carboxykinase 1 (PCK1), 17β-hydroxysteroid dehydrogenase type 13 (HSD17B13), carbohydrate-responsive element-binding protein (CHREBP), liver X receptor alpha (LXR α), transforming growth factor beta 1 (TGFB1), solute carrier family 25, member 4 (SCL25A4), Peroxisome proliferator-activated receptor-gamma coactivator 1 alpha (PGC1 α), cytokeratin 7 (CK7), cytokeratin 19 (CK19), hepatocyte nuclear factor 4 alpha (HNF4α), octamer-binding transcription factor 4 (OCT4), leucine-rich repeat containing G protein-coupled receptor 5 (LGR5), Albumin, and NANOG. All primers for qRT-PCR quantification were listed in Supplementary Table S1.

Statistical analysis

Statistical analyses were performed using GraphPad Prism 9.1.2 with Mann–Whitney test for non-paired samples. P values < 0.05 were considered as statistically significant.

Results

Lipid accumulation induced by lactate, pyruvate and octanoic acid in liver organoids

To model lipid accumulation in liver organoids, we adopted the protocol from a previous study based on exogenous supplementation of lactate (L), pyruvate (P), and octanoic acid (O) [16]. We used two concentrations defined as low and high concentration. We first tested in mouse liver organoids by adding LPO in the culture medium for 96 h (Supplemental Fig. S1A). We observed lipid accumulation in both low and high concentrations of LPO, but the induction level was moderate (Supplemental Fig. S1B-D). We next performed similar experiments in human ICOs (Fig. 1A and Supplementary Table S2). We observed that lipid accumulation in human liver organoids derived from three different donors was much more robust compared to that in mouse liver organoids (Fig. 1B). LPO exposure dose-dependently induced lipid deposition in human liver organoids shown by AdipoRed dye staining. Taking the organoids line DL1235 as an example, the average number of lipid droplets per cell in different groups was 18.90 ± 5.85 (control group without LPO), 38.53 ± 8.47 (low concentration of LPO), and 45.02 ± 11.56 (high concentration of LPO) (mean ± SEM, $n = 4$–6) (Fig. 1C). Consistently, lipid droplet sizes are significantly larger in LPO exposed organoids (Fig. 1D). In organoids line DL1235, the average of lipid droplet size in different groups was 0.23 ± 0.01 (control group without LPO), 0.90 ± 0.05 (low concentration of LPO), and 0.92 ± 0.05 (high concentration of LPO) (mean ± SEM, μm^2) (Fig. 1D). Of note, a sufficient concentration of LPO is required for lipid synthesis, as further diluting the low concentration by 10 to 100 times failed to induce lipid accumulation in human liver organoids (Supplemental Fig. S1E).

Another hallmark of fatty liver disease is excessive triglyceride accumulation in hepatocytes [17]. We found that LPO exposure significantly increased triglyceride level by $61.50 \pm 22.07\%$ (mean ± SEM, $n = 10$, $P < 0.01$) in human liver organoids, for example in the line DL1235, treated with

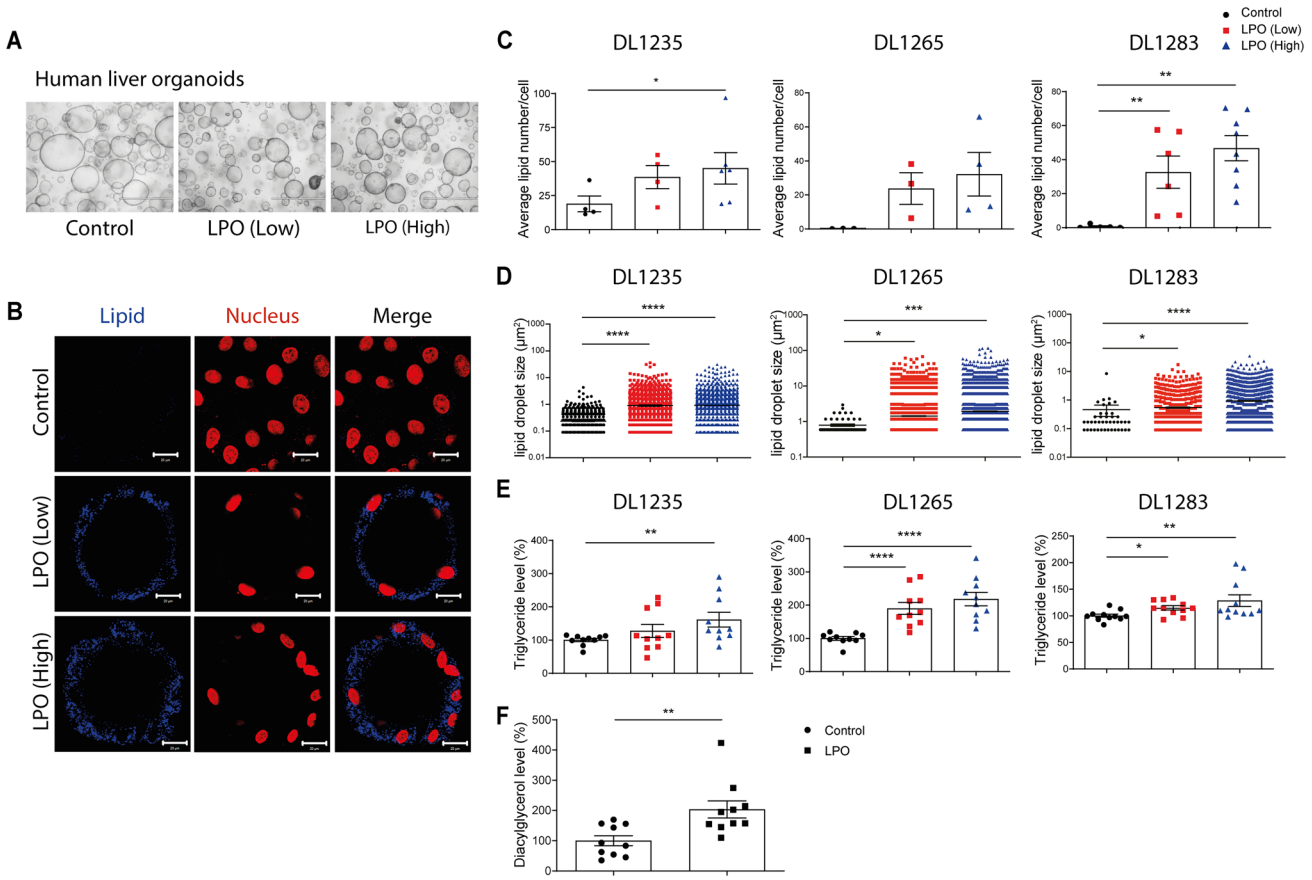

Fig. 1 Lipid accumulation in human liver organoids. **A** Morphology of human liver organoids cultured in expansion medium and exposed to LPO for 96 h. **B** Representative confocal images of lipid accumulation in human liver organoids with or without LPO treatment. Lipids were stained with AdipoRed (blue), and nuclei were marked by Hoechst (Red). **C** Average number of lipid droplets per cell in different organoids lines, DL1235 ($n=4$–6), DL1265 ($n=3$–4), DL1283 ($n=5$–8). **D** The size of all captured lipid droplets. The total captured number of lipid droplets in DL1235 are 1142, 1715, and 2071, respectively. The total captured number of lipid droplets in DL1265 are 64, 6465, 8507, respectively. The total captured number of lipid droplets in DL1283 are 42, 1534, 4539, respectively. **E** Triglyceride level with or without LPO treatment in different organoids lines, DL1235 ($n=10$), DL1265 ($n=10$), DL1283 ($n=11$). The triglyceride content was normalized to total protein concentration of the organoids. **F** Diacylglycerol level with or without LPO treatment in human liver organoids ($n=10$). The diacylglycerol content was normalized to total protein concentration of the organoids. (mean ± SEM; $*P<0.05$, $**P<0.01$, $***P<0.001$, $****P<0.0001$; Mann–Whitney test)

high concentration of LPO when compared with the control group (Fig. 1E). In addition, we found that diacylglycerol level was also increased by 103.5 ± 28.4% (mean ± SEM, $n=10$, $P<0.01$) in human liver organoids after LPO induction (Fig. 1F). Thus, 3D cultured liver organoids are capable of recapitulating lipid accumulation in vitro, but human compared with mouse liver organoids are much more robust in lipid deposition. Therefore, only human liver organoids were used in following experimentation.

Modeling excessive lipid accumulation in hepatocyte differentiated organoids

ICOs retain stemness and have the potential to differentiate toward the hepatocyte lineage culturing in hepatocyte differentiation medium [10, 12]. Interestingly, LPO exposure for 96 h significantly downregulated the expression of cholangiocyte markers (CK7 and CK19), whereas upregulated hepatocyte markers (Albumin and HNF4α) (Fig. 2A and B).

We next performed hepatocyte differentiation of ICOs by a well-defined culture medium [15]. Morphological appearance (Fig. 2C) and gene expression of representative markers (Supplemental Fig. S2) confirmed their hepatocyte-like phenotype. Importantly, both low and high concentrations of LPO supplementation resulted in lipid accumulation (Fig. 2D–G). The lipid droplet size (μm^2) in different groups was 0.89 ± 0.06 (control group without LPO), 2.54 ± 0.10 (low concentration of LPO), and 2.71 ± 0.08 (high concentration of LPO) (Fig. 2E). The average number of lipid droplets per cell in different groups was 0.72 ± 0.24

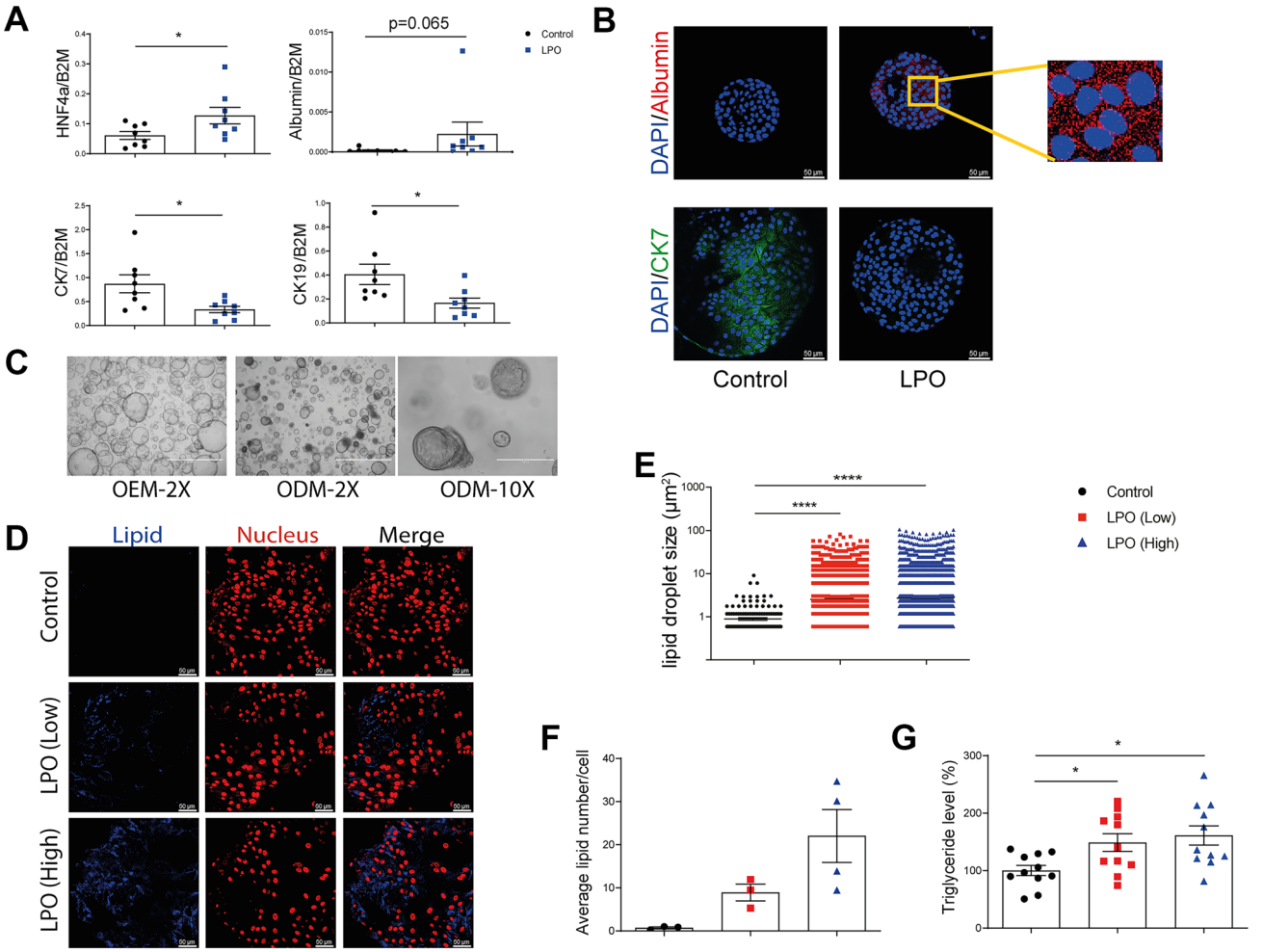

Fig. 2 Lipid accumulation in organoids differentiated toward hepatocyte-like phenotype. **A** ICOs were exposed to LPO, and mRNA expression levels of cholangiocytes and hepatocytes markers were quantified by qRT-PCR. CK7 and CK19 are cholangiocytes markers; Albumin and HNF4 α are hepatocytes markers, and B2M was used as reference gene ($n=8$). **B** Representative immunofluorescent images with DAPI/Albumin and CK7 staining are shown with or without LPO treatment. **C** Morphology of human liver organoids cultured in expansion medium and hepatocyte differentiation medium. *OEM* organoids expansion medium, *ODM* organoids differentiation medium. **D** Representative immunofluorescent images of lipid accumulation in differentiated organoids after LPO treatment with low concentration (L:P:O: 10 mM: 1 mM: 2 mM) and high concentration (L:P:O: 15 mM: 1.5 mM: 3 mM). Lipids marked by AdipoRed (blue); nuclei marked by Hoechst (Red). **E** The size of all captured lipid droplets. The total captured number of lipid droplets are 222, 3672, and 8122 respectively. **F** The average number of lipid droplets per cell ($n=3$–4). **G** Triglyceride level with or without LPO treatment ($n=11$). The triglyceride content was normalized to total protein concentration of the organoids. (mean ± SEM, $^{*}P<0.05$, $^{****}P<0.0001$; Mann–Whitney test)

(control group without LPO), 8.92 ± 1.93 (low concentration of LPO), and 22.06 ± 6.13 (high concentration of LPO) (mean ± SEM, $n=3$–4) (Fig. 2F). The triglyceride level increased by 48.70 ± 15.33% in low LPO group and 61.10 ± 16.83% in high LPO group, compared with control group without LPO exposure (mean ± SEM, $n=11$, $P<0.05$) (Fig. 2G). Similar results were confirmed in two other hepatocyte-differentiated organoid lines (Supplemental Fig. S3). The levels of lipid accumulation were comparable between differentiated and undifferentiated organoids, although there are some variations among different organoids lines (Supplemental Fig. S4). In addition, the expression of a panel of metabolic genes in differentiated and undifferentiated organoids was upregulated by LPO treatment (Supplemental Fig. S5). Even though different liver organoid lines can induce lipid accumulation in different culture medium with LPO exposure, it seems that organoids cultured in expansion medium format more lipid droplets than those organoids cultured in differentiation medium, while hepatocyte-like organoids deposit bigger lipid droplets.

Lipid accumulation moderately inhibits the growth of liver organoids

The growth characteristics of human ICOs were assessed by Alamar blue Assay 96 h after LPO exposure. Compared with control group, LPO dose-dependently but moderately inhibited organoids growth by 13.41 ± 1.62% at low and 19.13 ± 1.93% at high concentration (mean ± SEM, $n = 8$, $P < 0.001$) (Fig. 3A). The size of organoids cultured with LPO is significantly smaller than those cultured without LPO (Fig. 3B).

We next analyzed apoptosis and cell cycle by flow cytometry (Fig. 3C–F). We found LPO-induced apoptosis of organoid cells by 24.5 ± 2.45% with LPO exposure, while 14.82 ± 3.37% of apoptotic cells were detected in the control group (mean ± SEM, $n = 8$, $P < 0.01$) (Fig. 3C, D). Meanwhile, LPO exposure dose-dependently reduced the ratio of cells in S phase. There were 9.11 ± 2.30% at low and 6.37 ± 1.35% at high concentration, while 15.98 ± 2.43% cells of the control group were at S phase (mean ± SEM, $n = 6$, $P < 0.05$) (Fig. 3F). Our results suggest that LPO exposure moderately inhibits ICO growth possibly via inducing apoptosis and arresting cell cycle.

Genome-wide transcriptomic profiling reveals gene alternations of metabolic pathways and evidence of mitochondrial impairment by lipid accumulation

To map the global effects on gene transcription, we performed genome-wide transcriptomic analysis in human liver organoids exposed to LPO for 96 h. Volcano plot showed that 457 genes were significantly upregulated and 796 genes were downregulated (Fig. 4A). Heatmap showed the top 50 significantly differentially expressed genes comparing with and without LPO treatment (Fig. 4B). Kyoto encyclopedia of genes and genomes (KEGG) pathway analysis revealed that "metabolic pathways" are predominantly regulated involving 414 differentially expressed genes (Fig. 4C). This

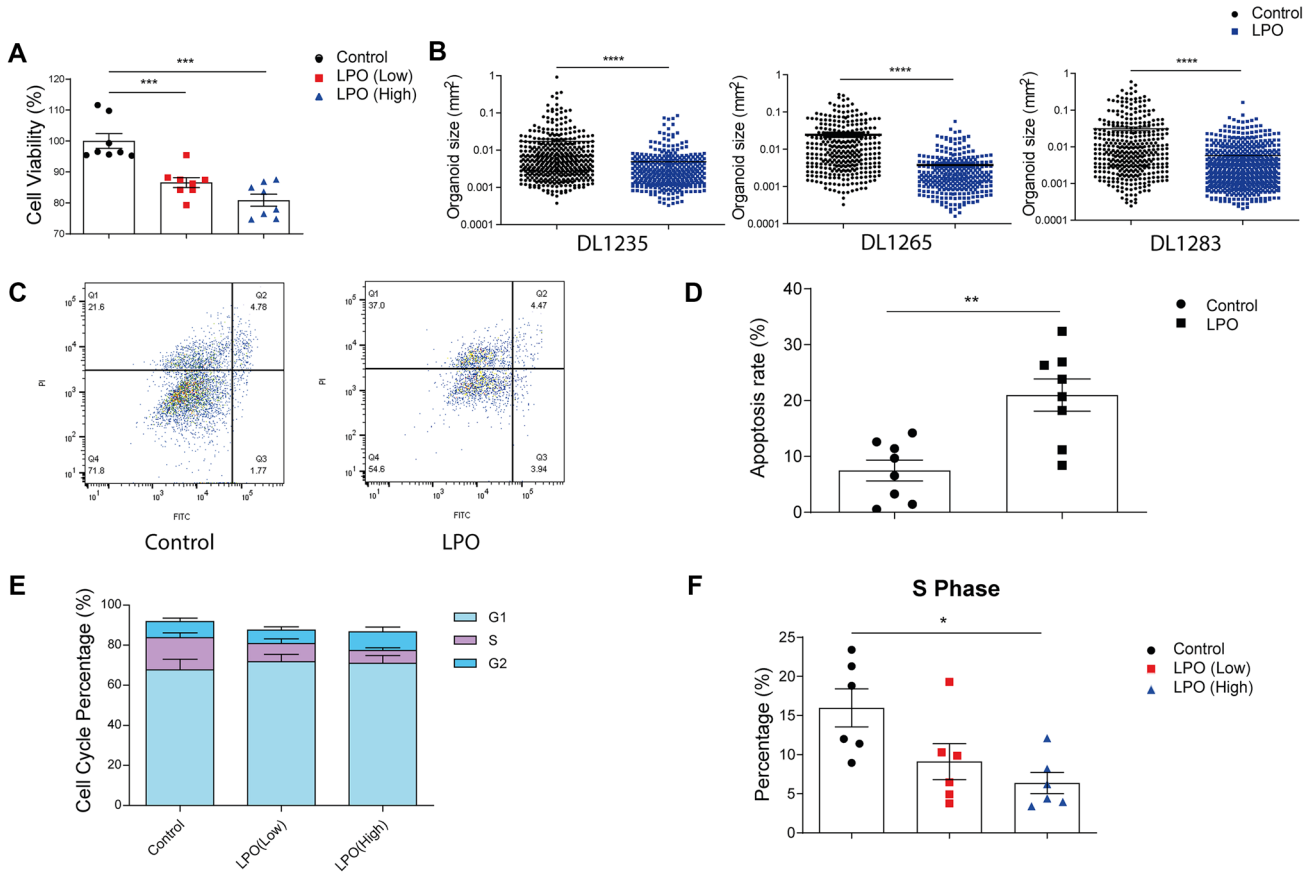

Fig. 3 The growth of human liver organoids after LPO treatment. **A** Cell viability of liver organoids ($n = 8$). **B** The size of liver organoids with LPO or without LPO treatment. The total captured number of organoids in DL1235 are 430 and 377. The total captured number of organoids in DL1265 are 330 and 304. The total captured number of organoids in DL1283 are 373 and 626. **C** Apoptosis in human liver organoids with or without LPO by analyzed flow cytometry. **D** The apoptosis rate in human liver organoids ($n = 8$). **E** Percentages of cells in different cell cycles ($n = 6$). **F** The percentage of liver organoids cells arrested in the S phase ($n = 6$). (mean ± SEM; $^{*}P < 0.05$, $^{**}P < 0.01$, $^{***}P < 0.001$, $^{****}P < 0.0001$; Mann–Whitney test)

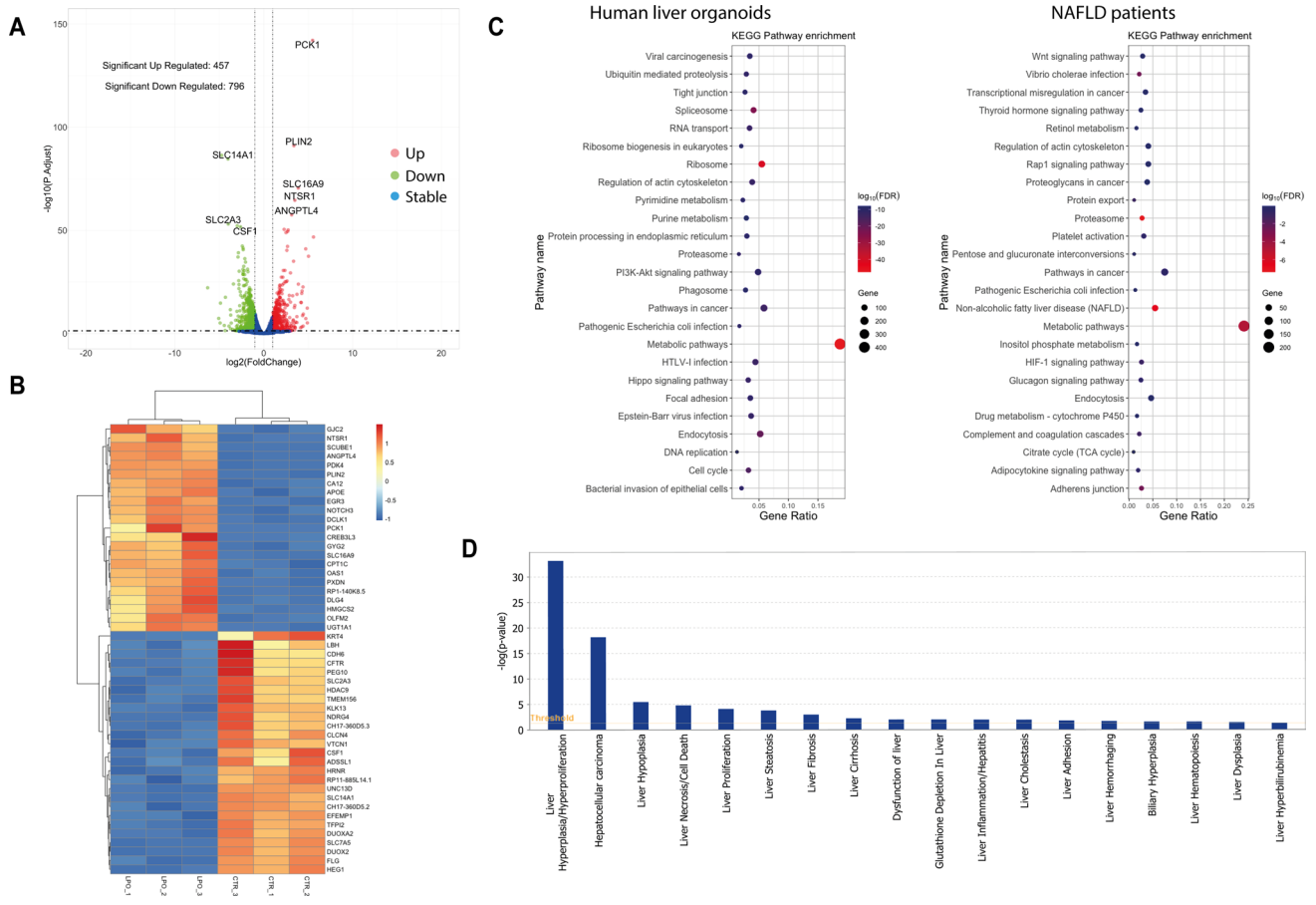

Fig. 4 Genome-wide transcriptomic analysis after LPO exposure. **A** Volcano plot of statistical significance ($P<0.05$) against fold change (ratio of LPO/Control group, $n=3$) of all the genes. **B** Heatmap showing top 50 differentially expressed genes. **C** KEGG pathway enrichment analysis using the complete set of significantly differentially expressed genes in organoids ($n=3$). Publically available data were retrieved (GSE126848) to compare the transcriptomes in liver tissues of NAFLD patients ($n=15$) with that of healthy controls ($n=14$). **D** Ingenuity Pathway Analysis based on significantly differentially regulated genes in the organoids model according to the module of "Liver diseases and functions"

is consistent with the analysis of transcriptomic data from liver issue of NAFLD patients (retrieved from GEO data sets GSE126848 [18]) (Fig. 4C). Ingenuity pathway analysis based on significantly differentially regulated genes revealed that "Liver steatosis" is among the top scored "Liver diseases and functions" (Fig. 4D).

Mitochondria essentially participate in cellular metabolism, and mitochondrial dysfunction has been commonly observed in fatty liver [19]. By stratifying genes encoded by mitochondrial DNA from the genome-wide transcriptomic analysis, we found a pattern of alteration comparing LPO treated and untreated organoids (Fig. 5A). Immunofluorescent co-staining showed enlarged mitochondria in lipid accumulated cells (Fig. 5B).

The increase of glucose level is also the hallmark of NAFLD phenotype, which is related to mitochondrial disorder. Thus, we tested glucose content in liver organoids with and without LPO treatment. We found that glucose level was increased after LPO treatment by $23.4 \pm 2.86\%$ (mean ± SEM, $n=18$, $P<0.0001$) (Fig. 5C). Mitochondria generate most of the cellular ATP through oxidative phosphorylation. ATP content is an index for mitochondrial function [20]. We found that LPO exposure and lipid accumulation resulted in significant reduction of ATP content by $71.22 \pm 3.87\%$ in DL1235, $79.58 \pm 3.85\%$ in DL1265, and $83.36 \pm 6.41\%$ in DL1283 (mean ± SEM, $n=6$–11, $P<0.001$) (Fig. 5D). These data collectively indicate metabolic dysregulation, in particular mitochondrial impairment, in liver organoids upon lipid accumulation.

The effects of obeticholic acid or metformin treatment on lipid deposition in organoids

To provide proof-of-concept that liver organoid-based fatty liver disease models are applicable of assessing novel therapeutics, we tested two drugs: obeticholic acid (INT747) and

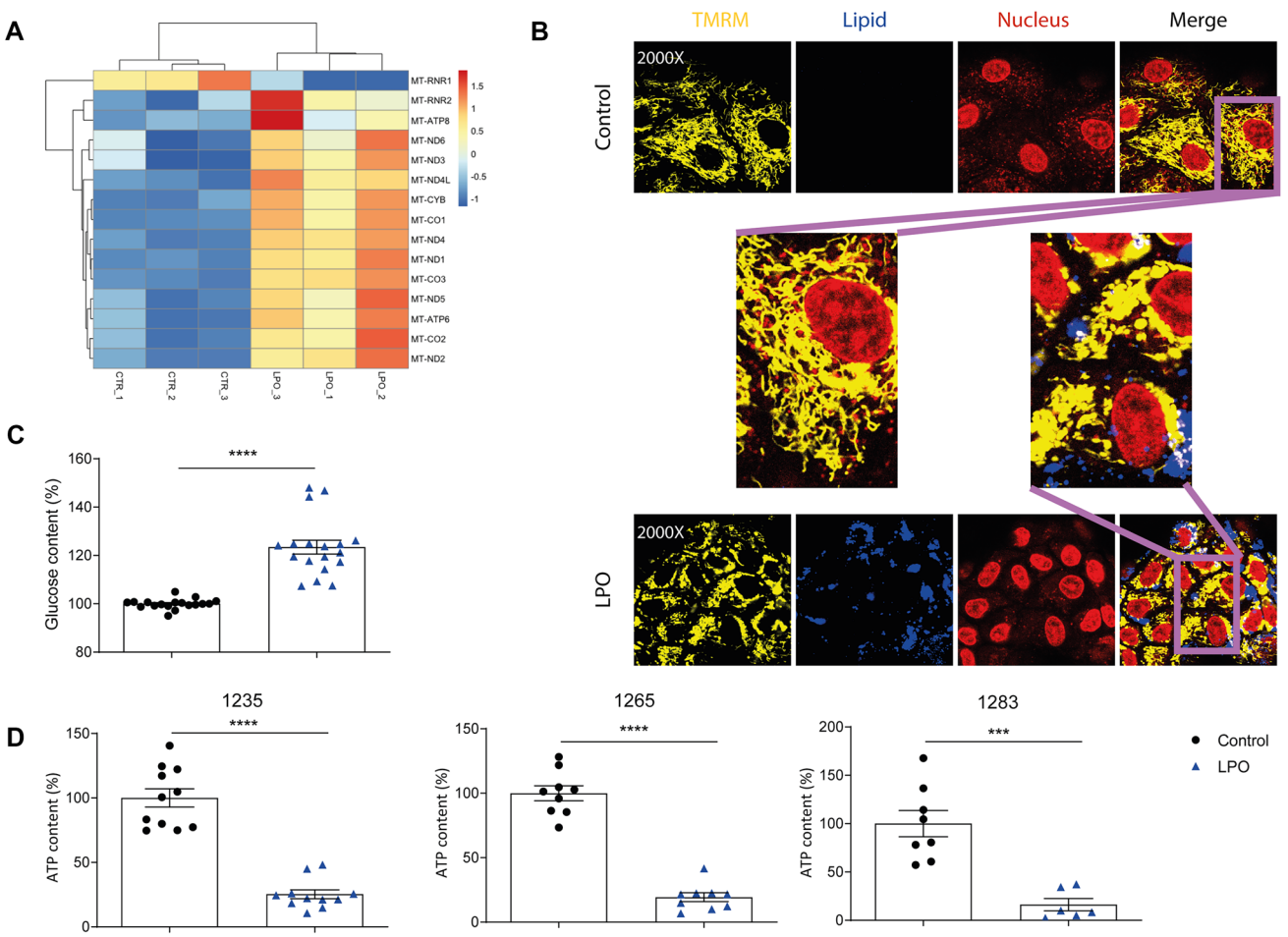

Fig. 5 Evidence of mitochondrial dysfunction in liver organoids upon lipid accumulation. **A** The expression pattern of mitochondrial encoded genes with or without LPO treatment, extracted from the genome-wide transcriptomic analysis. **B** Representative confocal images of mitochondria in organoids between control and LPO group. Mitochondria marked by TMRM (yellow); lipid droplets marked by MDH (blue); nuclei marked by DRAQ5 (Red). **C** Glucose content with or without LPO treatment ($n=18$). **D** ATP content in different organoids between control and LPO group, DL1235 ($n=11$), DL1265 ($n=9$), DL1283 ($n=6$–8). The glucose content and ATP content were normalized to total protein concentration of the organoids. (mean ± SEM, $^{***}P<0.001$, $^{****}P<0.0001$, Mann–Whitney test)

metformin. Obeticholic acid, a farnesoid X receptor agonist, has been reported to regulate hepatic metabolic homeostasis and improve liver steatosis [21, 22]. Metformin is an insulin sensitizer for type 2 diabetes treatment, which has been reported to reduce free fatty acids level and affect the development of MAFLD [23]. After 96 h exposure of LPO, we treated organoids with 1 μM INT 747 or metformin for 24 h, a relevant drug concentration as previously described [24–26]. We found INT 747 had mild effects on lipid droplet size that significant reduction was observed in three but not the other organoids line (Fig. 6). Metformin significantly but moderately reduced lipid droplet size in both tested organoids lines (Fig. 7). These demonstrated a proof-of-concept of testing medications on lipid accumulation.

Discussion

Fatty liver disease has grown into a major global health issue, but there is no specific treatment available. Advancing research and therapeutic development requires robust experimental models that can resemble the disease as seen in patients. Mouse models have been widely used to study the pathogenesis of fatty liver disease and assess therapeutic interventions. Although these models have unique advantages that can capture not only steatosis, but also the pathogenic process of inflammation and fibrosis [23], they have major limitations in particular given the obvious species barrier. Thus, experimental models of human origin remain essentially required. Currently, immortalized human liver

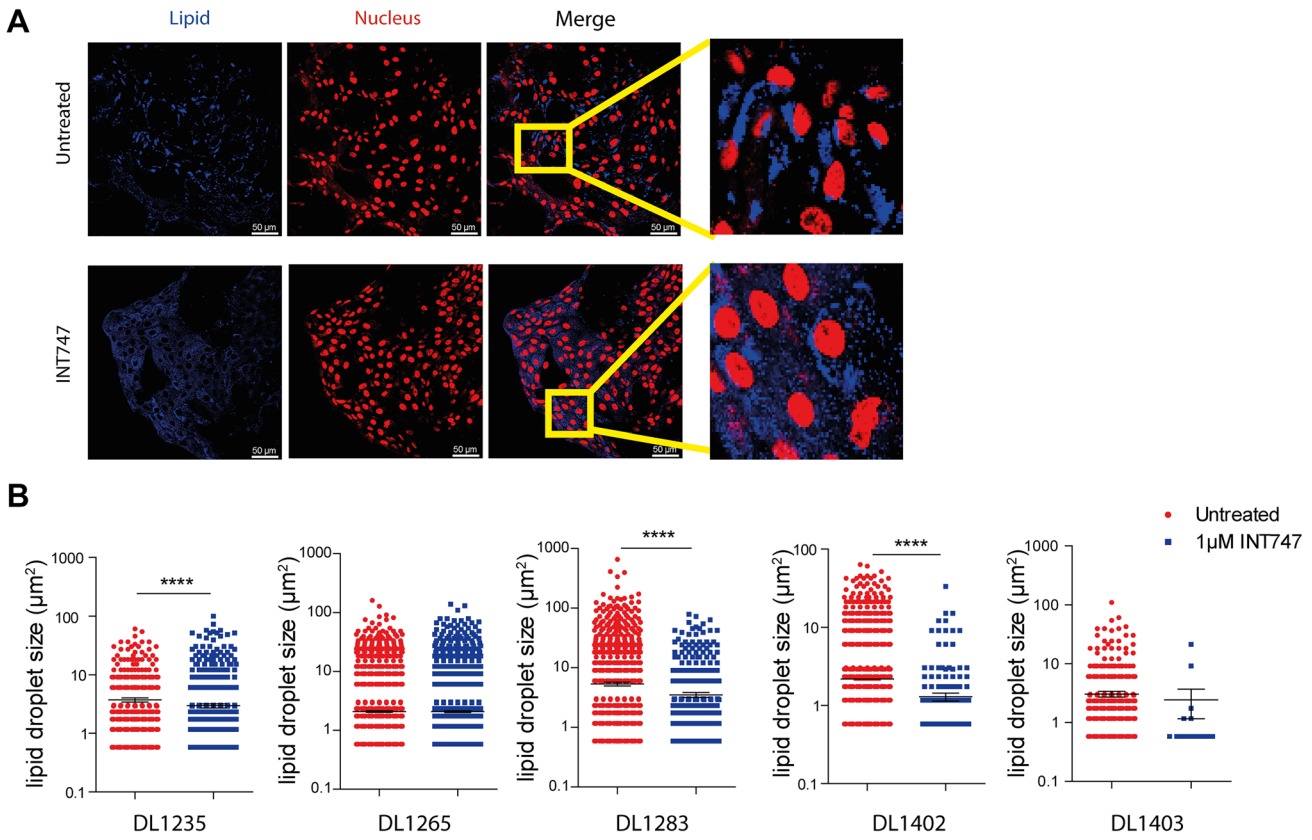

Fig. 6 Treatment with INT747 reduce lipid accumulation in organoids cultured in expansion medium. **A** Representative confocal images of lipid accumulation in undifferentiated organoids treated or untreated with INT747 (lipids: blue; nuclei: red). **B** Lipid droplet size between untreated and INT747 treated in five different liver organoids exposed to LPO. The total captured number of lipid droplets in DL1235 are 524 and 1000, respectively. The total captured number of lipid droplets in DL1265 are 6442 and 6312, respectively. The total captured number of lipid droplets in DL1402 are 3563 and 310, respectively. The total captured number of lipid droplets in DL1403 are 536 and 17, respectively. (mean ± SEM, ****$P < 0.0001$, Mann–Whitney test)

cancer lines including HepG2, Huh7, and HepRG have been explored to establish in vitro models for fatty liver disease. These cell culture models primarily capture steatosis, one hallmark of fatty liver disease. Through exposure to free fatty acids treatment, these cells can capture the process of lipid accumulation in a 2D cell culture setting [27–29]. However, these immortalized malignant cells harbor numerous genetic and functional alterations that compromise the authenticity in modeling fatty liver disease, a non-malignant disease. Primary human hepatocytes are the ideal cell type in this respect, but these cells are technically difficult to be cultured and maintained for experimentation. Hepatocyte-like cells differentiated from induced pluripotent stem cells or embryonic stem cells have been used as an alternative and are capable of modeling lipid accumulation [30].

The recent development of organoids technology has provided a unique opportunity to further advance in vitro models of fatty liver disease. The liver harbors residential progenitor cells that can be cultured into organoids with cholangiocyte phenotype. 3D organoid cultures have also been successfully generated from single hepatocytes and can grow for several months in vitro [14], but there are remaining technical challenges for wide applications. Using a different approach, a recent study has generated hepatic organoids from human embryonic stem cells and induced pluripotent stem cells. These organoids contain a higher proportion of hepatocytes to cholangiocytes, and can accumulate lipids when exposed to free fatty acids [8]. However, these organoids are prone to accumulate genomic and epigenomic alterations [31, 32], whereas organoids derived from primary adult liver stem cells are genetically more stable [10]. In this study, we successfully recapitulated excessive lipid accumulation in human adult liver-derived organoids by exogenous supplementation of lactate (L), pyruvate (P), and octanoic acid (O), an approach that better mimics de novo lipid synthesis compared to free fatty acids exposure [16]. Lactate and pyruvate are physiological substrates of both gluconeogenesis and de novo lipogenesis. Octanoic acid, as a form of medium chain fatty acid, can more effectively induce triglyceride accumulation, compared to long chain

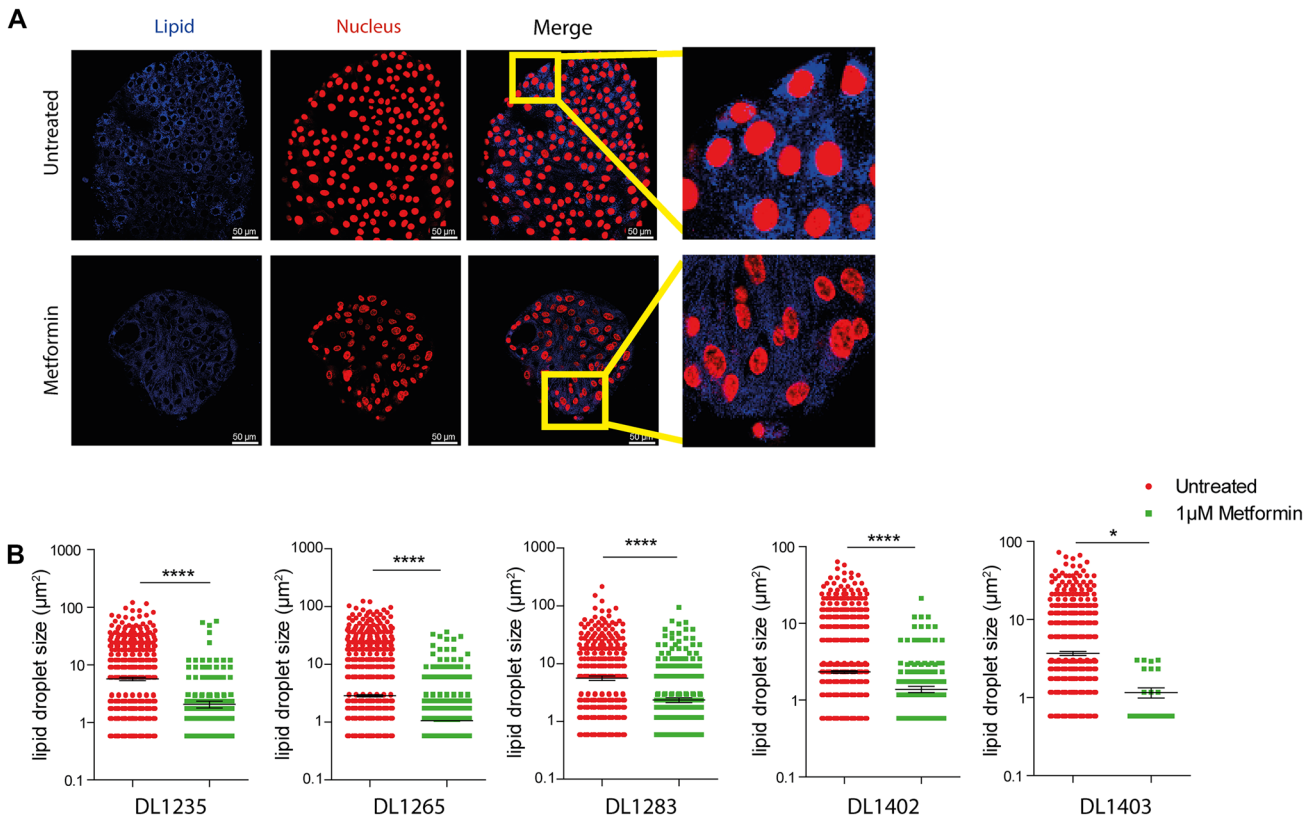

Fig. 7 Treatment with metformin reduce lipid accumulation in organoids cultured in expansion medium. **A** Representative confocal images of lipid accumulation between untreated and metformin treated organoids (lipids: blue; nuclei: red). **B** Lipid droplet size of liver organoids exposed LPO between untreated and metformin treated, in five different liver organoids lines. The total captured number of lipid droplets in DL1235 are 1083 and 383, respectively. The total captured number of lipid droplets in DL1265 are 4512 and 3546, respectively. The total captured number of lipid droplets in DL1283 are 848 and 808 respectively. The total captured number of lipids in DL1402 are 2635 and 291, respectively. The total captured number of lipid droplets in DL1403 are 1219 and 29, respectively. (mean ± SEM, $*P < 0.05$, $****P < 0.0001$, Mann–Whitney test)

fatty acids, such as oleate [33]. The combination of lactate, pyruvate and octanoic acid enhance tricarboxylic acid cycle (TCA) activity, leading to the increase of mitochondrial respiration. We found liver organoids cultured from human compared to mouse liver tissue were much better in lipid accumulation when exposed to LPO. This is consistent with a previous study showing that liver organoids of feline and human compared with those of dog and mouse origin are more efficient in accumulating lipids when treated with free fatty acids including oleate and palmitate [34]. Thus, in this study, we primarily focused on the use of human liver organoids. Of note, our liver organoids are derived from intrahepatic bile ducts with cholangiocyte-like phenotype. However, in patients with fatty liver disease, hepatocytes are the main cell type accumulating lipids [3]. We thus have differentiated our ICOs into hepatocytes-like cells, and they were also capable of accumulating lipids. It would be interesting to comparatively study the use of different types of liver organoids for modeling steatosis in future research.

The liver displays regenerative capacity after surgical resection or injury. Liver organoids derived from intrahepatic bile ducts consist of bipotent progenitors [35]. Even though there is no mature hepatocytes in ICOs, progenitors express some hepatocyte markers and have the potential to differentiate toward hepatocytes [10, 15]. In the existing models, hepatocytes are the main object of NAFLD studies. However, progenitors are also involved in NAFLD progression. Progenitors/stem cells are activated and preferentially differentiate toward hepatocytes both in NAFLD animal models and in patients [36–38]. These results are consistent with our findings that LPO exposure upregulates hepatocyte markers in ICOs. Recent studies suggest that lipid metabolic states regulate the fate of progenitors to self-renew or differentiation [39]. Proliferating retinal stem cells showed enriched saturated fatty acids than differentiated retinal cells [40]. The shift of quiescence and proliferation of neural stem/progenitor cells regulated by fatty acid oxidation [41]. Thus, the exact role of lipid metabolism in different

cell types derived from liver organoids is interesting to be further studied.

Patients with fatty liver disease are often accompanied with metabolic disorders, which in turn aggravate the progression of fatty liver disease [42, 43]. The new term, MAFLD, emphasizes metabolic dysfunctions, including the presence of type II diabetes mellitus, overweight/obesity or minimal two minor metabolic abnormalities. In cell culture models, exposure to LPO compared with free fatty acids is much better in recapitulating metabolic dysregulation and the expression of metabolism-associated genes [30]. Mitochondria, the powerhouse of cells, essentially regulate metabolism and play an important role in the pathogenesis of fatty liver disease [19]. It has been shown that LPO treatment enhances mitochondrial respiration and reactive oxygen species formation during lipid accumulation [5, 44]. In our organoids model, lipid accumulation regulates over 400 genes that are attributed to metabolic pathways. Furthermore, we provided evidence of mitochondrial dysfunction induced by lipid accumulation. To further advance the model system, it would be important to incorporate different cell types to also recapitulate inflammatory response and fibrogenesis, in addition to lipid accumulation. A previous study has demonstrated proof-of-concept that liver organoids generated from pluripotent stem cell lines compose of hepatocyte-, stellate-, and Kupffer-like cells that recapitulate several features of fatty liver disease, including steatosis, inflammation, and fibrosis phenotypes [7].

Although no approved medication is available, there are several pipeline drugs at clinical development stage for treating fatty liver disease. These drugs are primarily aimed at reversing hepatic fibrosis or anti-inflammation [45]. Obeticholic acid (INT747), a natural Farnesoid X receptor agonist, has been demonstrated to significantly improved fibrosis in a large phase 3 trial [46]. In our model, INT747 treatment appears to have mild effect on lipid synthesis, which is consistent with its mechanism-of-action that is not primarily targeting lipid synthesis. Metformin is the first-line medication for treating type 2 diabetes. The effects on the development and progression of MAFLD has been widely implicated, but remain highly controversial [47]. In liver organoids, we found that metformin treatment significantly but moderately inhibited LPO-induced lipid accumulation, which may help to understand the underlying mechanism how metformin affects fatty liver disease. This provided proof-of-concept that our organoids model bears usefulness for therapeutic development.

In summary, this study has successfully established liver organoids-based models in recapitulating excessive lipid accumulation and associated metabolic dysregulation. This shall provide an innovative tool for studying pathogenesis and developing therapeutics for treating fatty liver disease. Here, we only recapitulate lipid accumulation but not inflammation and fibrosis. Adding immune and stromal cell compartments into organoids may help to further advance the model to better capture the pathogenic spectrum of fatty liver disease. Future research is warranted to further improve the model for better recapitulating the critical features of the disease.

Supplementary Information The online version contains supplementary material available at https://doi.org/10.1007/s00109-021-02176-x.

Author contribution Ling Wang, Meng Li, Jiaye Liu, Ruiyi Zhang, and Ibrahim Ayada performed the experimental studies. Ling Wang and Meng Li analyzed the experimental data. Bingting Yu performed the bioinformatics analysis. Luc J. W. van der Laan, Monique M. A. Verstegen, and Shaojun Shi provided the organoids lines with technical support. Maikel P. Peppelenbosch, Wanlu Cao, and Qiuwei Pan contributed to study design and supervision. The first draft of the manuscript was written by Ling Wang and all authors edited the manuscript. All authors read and approved the final manuscript.

Funding This research is supported by a VIDI grant (No. 91719300) from the Netherlands Organisation for Scientific Research (to Q. Pan), the Dutch Cancer Society for funding a Dutch Cancer Society Young Investigator Grant (10140) to Q. Pan, and China Scholarship Council for funding PhD fellowships to L. Wang (No.201708530248), S. Shi (No.201706230252) and R. Zhang (No.201808530490).

Data availability All data generated or analyzed during this study are included in this published article and its supplementary information files.

Declarations

Ethical approval and consent to participate The experiment used of liver tissues for organoids research was approved by the Medical Ethical Council of the Erasmus MC ((MEC2006-202) and patient informed consent was given.

Competing interests The authors declare no competing interests.

References

1. Vernon G, Baranova A, Younossi ZM (2011) Systematic review: the epidemiology and natural history of non-alcoholic fatty liver disease and non-alcoholic steatohepatitis in adults. Aliment Pharmacol Ther 34:274–285. https://doi.org/10.1111/j.1365-2036.2011.04724.x
2. Eslam M, Newsome PN, Sarin SK, Anstee QM, Targher G, Romero-Gomez M, Zelber-Sagi S, Wong VWS, Dufour J-F, Schattenberg JM et al (2020) A new definition for metabolic dysfunction-associated fatty liver disease: an international expert consensus statement. J Hepatol 73:202–209. https://doi.org/10.1016/j.jhep.2020.03.039
3. Wang L, Liu J, Miao Z, Pan Q, Cao W (2021) Lipid droplets and their interactions with other organelles in liver diseases. Int J Biochem Cell Biol 133:105937. https://doi.org/10.1016/j.biocel.2021.105937
4. Yang P, Wang Y, Tang W, Sun W, Ma Y, Lin S, Jing J, Jiang L, Shi H, Song Z et al (2020) Western diet induces severe nonalcoholic

steatohepatitis, ductular reaction, and hepatic fibrosis in liver CGI-58 knockout mice. Sci Rep 10:4701. https://doi.org/10.1038/s41598-020-61473-6
5. Lockman KA, Htun V, Sinha R, Treskes P, Nelson LJ, Martin SF, Rogers SM, Le Bihan T, Hayes PC, Plevris JN (2016) Proteomic profiling of cellular steatosis with concomitant oxidative stress in vitro. Lipids Health Dis 15:114. https://doi.org/10.1186/s12944-016-0283-7
6. Yu K, Chen B, Aran D, Charalel J, Yau C, Wolf DM, van't Veer LJ, Butte AJ, Goldstein T, Sirota M (2019) Comprehensive transcriptomic analysis of cell lines as models of primary tumors across 22 tumor types. Nat Commun 10:3574. https://doi.org/10.1038/s41467-019-11415-2
7. Ouchi R, Togo S, Kimura M, Shinozawa T, Koido M, Koike H, Thompson W, Karns RA, Mayhew CN, McGrath PS et al (2019) Modeling steatohepatitis in humans with pluripotent stem cell-derived organoids. Cell Metab 30:374–384. https://doi.org/10.1016/j.cmet.2019.05.007
8. Ramli MNB, Lim YS, Koe CT, Demircioglu D, Tng W, Gonzales KAU, Tan CP, Szczerbinska I, Liang H, Soe EL et al (2020) Human pluripotent stem cell-derived organoids as models of liver disease. Gastroenterology 159:1471–1486. https://doi.org/10.1053/j.gastro.2020.06.010
9. Dutta D, Heo I, Clevers H (2017) Disease modeling in stem cell-derived 3D organoid systems. Trends Mol Med 23:393–410. https://doi.org/10.1016/j.molmed.2017.02.007
10. Huch M, Gehart H, van Boxtel R, Hamer K, Blokzijl F, Verstegen Monique MA, Ellis E, van Wenum M, Fuchs Sabine A, de Ligt J et al (2015) Long-term culture of genome-stable bipotent stem cells from adult human liver. Cell 160:299–312. https://doi.org/10.1016/j.cell.2014.11.050
11. Cao W, Chen K, Bolkestein M, Yin Y, Verstegen MMA, Bijvelds MJC, Wang W, Tuysuz N, ten Berge D, Sprengers D et al (2017) Dynamics of Proliferative and Quiescent Stem Cells in Liver Homeostasis and Injury. Gastroenterology 153:1133–1147. https://doi.org/10.1053/j.gastro.2017.07.006
12. Verstegen MMA, Roos FJM, Burka K, Gehart H, Jager M, de Wolf M, Bijvelds MJC, de Jonge HR, Ardisasmita AI, van Huizen NA et al (2020) Human extrahepatic and intrahepatic cholangiocyte organoids show region-specific differentiation potential and model cystic fibrosis-related bile duct disease. Sci Rep 10:21900. https://doi.org/10.1038/s41598-020-79082-8
13. Marsee A, Roos FJM, Verstegen MMA, Marsee A, Roos F, Verstegen M, Clevers H, Vallier L, Takebe T, Huch M et al (2021) Building consensus on definition and nomenclature of hepatic, pancreatic, and biliary organoids. Cell Stem Cell 28:816–832. https://doi.org/10.1016/j.stem.2021.04.005
14. Hu H, Gehart H, Artegiani B, Löpez-Iglesias C, Dekkers F, Basak O, van Es J, de Sousa Lopes SMC, Begthel H, Korving J et al (2018) Long-term expansion of functional mouse and human hepatocytes as 3D organoids. Cell 175:1591–1606. https://doi.org/10.1016/j.cell.2018.11.013
15. Broutier L, Andersson-Rolf A, Hindley CJ, Boj SF, Clevers H, Koo B-K, Huch M (2016) Culture and establishment of self-renewing human and mouse adult liver and pancreas 3D organoids and their genetic manipulation. Nat Protoc 11:1724–1743. https://doi.org/10.1038/nprot.2016.097
16. Lyall MJ, Cartier J, Thomson JP, Cameron K, Meseguer-Ripolles J, O'Duibhir E, Szkolnicka D, Villarin BL, Wang Y, Blanco GR et al (2018) Modelling non-alcoholic fatty liver disease in human hepatocyte-like cells. Philos Trans R Soc Lond B Biol Sci 373:20170362. https://doi.org/10.1098/rstb.2017.0362
17. Yamaguchi K, Yang L, McCall S, Huang J, Yu XX, Pandey SK, Bhanot S, Monia BP, Li Y-X, Diehl AM (2007) Inhibiting triglyceride synthesis improves hepatic steatosis but exacerbates liver damage and fibrosis in obese mice with nonalcoholic steatohepatitis. Hepatology 45:1366–1374. https://doi.org/10.1002/hep.21655
18. Suppli MP, Rigbolt KTG, Veidal SS, Heebøll S, Eriksen PL, Demant M, Bagger JI, Nielsen JC, Oró D, Thrane SW et al (2019) Hepatic transcriptome signatures in patients with varying degrees of non-alcoholic fatty liver disease compared with healthy normal-weight individuals. Am J Physiol Gastrointest Liver Physiol 316:G462–G472. https://doi.org/10.1152/ajpgi.00358.2018
19. Rector RS, Thyfault JP, Uptergrove GM, Morris EM, Naples SP, Borengasser SJ, Mikus CR, Laye MJ, Laughlin MH, Booth FW et al (2010) Mitochondrial dysfunction precedes insulin resistance and hepatic steatosis and contributes to the natural history of non-alcoholic fatty liver disease in an obese rodent model. J Hepatol 52:727–736. https://doi.org/10.1016/j.jhep.2009.11.030
20. Dornas W, Schuppan D (2020) Mitochondrial oxidative injury: a key player in nonalcoholic fatty liver disease. Am J Physiol Gastrointest Liver Physiol 319:G400–G411. https://doi.org/10.1152/ajpgi.00121.2020
21. Jiao Y, Lu Y, Li X-Y (2015) Farnesoid X receptor: a master regulator of hepatic triglyceride and glucose homeostasis. Acta Pharmacol Sin 36:44–50. https://doi.org/10.1038/aps.2014.116
22. de Oliveira MC, Gilglioni EH, de Boer BA, Runge JH, de Waart DR, Salgueiro CL, Ishii-Iwamoto EL, Oude Elferink RPJ, Gaemers IC (2016) Bile acid receptor agonists INT747 and INT777 decrease oestrogen deficiency-related postmenopausal obesity and hepatic steatosis in mice. Biochim Biophys Acta Mol Basis Dis 1862:2054–2062. https://doi.org/10.1016/j.bbadis.2016.07.012
23. Brandt A, Hernández-Arriaga A, Kehm R, Sánchez V, Jin CJ, Nier A, Baumann A, Camarinha-Silva A, Bergheim I (2019) Metformin attenuates the onset of non-alcoholic fatty liver disease and affects intestinal microbiota and barrier in small intestine. Sci Rep 9:6668. https://doi.org/10.1038/s41598-019-43228-0
24. Verbeke L, Farre R, Trebicka J, Komuta M, Roskams T, Klein S, Elst IV, Windmolders P, Vanuytsel T, Nevens F et al (2014) Obeticholic acid, a farnesoid X receptor agonist, improves portal hypertension by two distinct pathways in cirrhotic rats. Hepatology 59:2286–2298. https://doi.org/10.1002/hep.26939
25. Kajbaf F, De Broe ME, Lalau J-D (2016) Therapeutic concentrations of metformin: a systematic review. Clin Pharmacokinet 55:439–459. https://doi.org/10.1007/s40262-015-0323-x
26. Kinaan M, Ding H, Triggle CR (2015) Metformin: an old drug for the treatment of diabetes but a new drug for the protection of the endothelium. Med Princ Pract 24:401–415. https://doi.org/10.1159/000381643
27. Gómez-Lechón MJ, Donato MT, Martínez-Romero A, Jiménez N, Castell JV, O'Connor J-E (2007) A human hepatocellular in vitro model to investigate steatosis. Chem Biol Interact 165:106–116. https://doi.org/10.1016/j.cbi.2006.11.004
28. Michaut A, Le Guillou D, Moreau C, Bucher S, McGill MR, Martinais S, Gicquel T, Morel I, Robin M-A, Jaeschke H et al (2016) A cellular model to study drug-induced liver injury in nonalcoholic fatty liver disease: Application to acetaminophen. Toxicol Appl Pharmacol 292:40–55. https://doi.org/10.1016/j.taap.2015.12.020
29. Takahara I, Akazawa Y, Tabuchi M, Matsuda K, Miyaaki H, Kido Y, Kanda Y, Taura N, Ohnita K, Takeshima F et al (2017) Toyocamycin attenuates free fatty acid-induced hepatic steatosis and apoptosis in cultured hepatocytes and ameliorates nonalcoholic fatty liver disease in mice. PLoS One 12:e0170591. https://doi.org/10.1371/journal.pone.0170591
30. Graffmann N, Ring S, Kawala M-A, Wruck W, Ncube A, Trompeter H-I, Adjaye J (2016) Modeling nonalcoholic fatty liver disease with human pluripotent stem cell-derived immature hepatocyte-like cells reveals activation of PLIN2 and confirms regulatory functions of peroxisome proliferator-activated receptor alpha. Stem Cells Dev 25:1119–1133. https://doi.org/10.1089/scd.2015.0383

31. Pera MF (2011) The dark side of induced pluripotency. Nature 471:46–47. https://doi.org/10.1038/471046a
32. Liang G, Zhang Y (2013) Genetic and epigenetic variations in iPSCs: potential causes and implications for application. Cell Stem Cell 13:149–159. https://doi.org/10.1016/j.stem.2013.07.001
33. Guo W, Choi JK, Kirkland JL, Corkey BE, Hamilton JA (2000) Esterification of free fatty acids in adipocytes: a comparison between octanoate and oleate. Biochem J 349:463–471. https://doi.org/10.1042/0264-6021:3490463
34. Kruitwagen HS, Oosterhoff LA, Vernooij IGWH, Schrall IM, van Wolferen ME, Bannink F, Roesch C, van Uden L, Molenaar MR, Helms JB et al (2017) Long-term adult feline liver organoid cultures for disease modeling of hepatic steatosis. Stem Cell Rep 8:822–830. https://doi.org/10.1016/j.stemcr.2017.02.015
35. Prior N, Inacio P, Huch M (2019) Liver organoids: from basic research to therapeutic applications. Gut 68:2228. https://doi.org/10.1136/gutjnl-2019-319256
36. Nobili V, Carpino G, Alisi A, Franchitto A, Alpini G, De Vito R, Onori P, Alvaro D, Gaudio E (2012) Hepatic progenitor cells activation, fibrosis, and adipokines production in pediatric non-alcoholic fatty liver disease. Hepatology 56:2142–2153. https://doi.org/10.1002/hep.25742
37. Paku S, Nagy P, Kopper L, Thorgeirsson SS (2004) 2-acetylaminofluorene dose-dependent differentiation of rat oval cells into hepatocytes: Confocal and electron microscopic studies. Hepatology 39:1353–1361. https://doi.org/10.1002/hep.20178
38. Raven A, Lu W-Y, Man TY, Ferreira-Gonzalez S, O'Duibhir E, Dwyer BJ, Thomson JP, Meehan RR, Bogorad R, Koteliansky V et al (2017) Cholangiocytes act as facultative liver stem cells during impaired hepatocyte regeneration. Nature 547:350–354. https://doi.org/10.1038/nature23015
39. Clémot M, Sênos Demarco R, Jones DL (2020) Lipid mediated regulation of adult stem cell behavior. Front Cell Dev Biol 8:115. https://doi.org/10.3389/fcell.2020.00115
40. Li J, Cui Z, Zhao S, Sidman RL (2007) Unique glycerophospholipid signature in retinal stem cells correlates with enzymatic functions of diverse long-chain acyl-CoA synthetases. Stem Cells 25:2864–2873. https://doi.org/10.1634/stemcells.2007-0308
41. Knobloch M, Pilz G-A, Ghesquière B, Kovacs WJ, Wegleiter T, Moore DL, Hruzova M, Zamboni N, Carmeliet P, Jessberger S (2017) A fatty acid oxidation-dependent metabolic shift regulates adult neural stem cell activity. Cell Rep 20:2144–2155. https://doi.org/10.1016/j.celrep.2017.08.029
42. Yki-Järvinen H (2014) Non-alcoholic fatty liver disease as a cause and a consequence of metabolic syndrome. Lancet Diabetes Endocrinol 2:901–910. https://doi.org/10.1016/s2213-8587(14)70032-4
43. Yang KC, Hung H-F, Lu C-W, Chang H-H, Lee L-T, Huang K-C (2016) Association of non-alcoholic fatty liver disease with metabolic syndrome independently of central obesity and insulin resistance. Sci Rep 6:27034. https://doi.org/10.1038/srep27034
44. Lockman KA, Baren JP, Pemberton CJ, Baghdadi H, Burgess KE, Plevris-Papaioannou N, Lee P, Howie F, Beckett G, Pryde A et al (2012) Oxidative stress rather than triglyceride accumulation is a determinant of mitochondrial dysfunction in in vitro models of hepatic cellular steatosis. Liver Int 32:1079–1092. https://doi.org/10.1111/j.1478-3231.2012.02775.x
45. Dufour J-F, Caussy C, Loomba R (2020) Combination therapy for non-alcoholic steatohepatitis: rationale, opportunities and challenges. Gut 69:1877. https://doi.org/10.1136/gutjnl-2019-319104
46. Younossi ZM, Ratziu V, Loomba R, Rinella M, Anstee QM, Goodman Z, Bedossa P, Geier A, Beckebaum S, Newsome PN et al (2019) Obeticholic acid for the treatment of non-alcoholic steatohepatitis: interim analysis from a multicentre, randomised, placebo-controlled phase 3 trial. Lancet 394:2184–2196. https://doi.org/10.1016/S0140-6736(19)33041-7
47. Jalali M, Rahimlou M, Mahmoodi M, Moosavian SP, Symonds ME, Jalali R, Zare M, Imanieh MH, Stasi C (2020) The effects of metformin administration on liver enzymes and body composition in non-diabetic patients with non-alcoholic fatty liver disease and/or non-alcoholic steatohepatitis: An up-to date systematic review and meta-analysis of randomized controlled trials. Pharmacol Res 159:104799. https://doi.org/10.1016/j.phrs.2020.104799